360 keV could have any significant effect on the differential cross sections above 400 keV, even if Γ_d/Γ should be large for this resonance, because of the quoted width, $\Gamma<2$ keV.

ACKNOWLEDGMENTS

The author wishes to express his gratitude to Professor C. A. Barnes for his assistance and guidance during the course of this experiment. The advice and support of Professor R. F. Christy, Professor W. A. Fowler, Professor R. W. Kavanagh, Professor T. Lauritsen, Professor H. A. Weidenmüller, and Professor W. Whaling have been appreciated. The aid of Mrs. B. A. Zimmerman in the programming and operation of the electronic computer used for many of the calculations is gratefully acknowledged.

PHYSICAL REVIEW VOLUME 136, NUMBER 4B 23 NOVEMBER 1964

Elastic Scattering of Deuterons by Ca^{40}†

R. H. Bassel, R. M. Drisko, and G. R. Satchler
Oak Ridge National Laboratory, Oak Ridge, Tennessee

AND

L. L. Lee, Jr., J. P. Schiffer, and B. Zeidman
Argonne National Laboratory, Argonne, Illinois

(Received 6 July 1964)

The elastic scattering from Ca^{40} of deuterons with energies of 7, 8, 9, 10, 11, and 12 MeV has been measured and subjected to optical-model analysis, as a preliminary to a distorted-wave study of the $Ca^{40}(d,p)$ reaction. Considerable ambiguities in the optical-model parameters are found, and the results are discussed in detail. Inclusion of a polarization potential and of spin-orbit coupling is found to have little effect. An attempt is made to find a set of parameters that gives a good over-all fit at all the energies.

I. INTRODUCTION

THE usefulness of reactions such as deuteron stripping as sources of information about nuclear structure has been enhanced in recent years by the introduction of analysis by the distorted-wave Born approximation. A prerequisite for the application of this theory is a knowledge of the *elastic* scattering of the particles involved. In practice, this scattering is analyzed in terms of an optical-model potential, which is used to generate the distorted waves in the reaction calculation.

The present measurement and analysis of the scattering of deuterons by Ca^{40} at energies from 7 to 12 MeV was undertaken as a preliminary to a detailed study of the validity of the distorted-wave theory for the deuteron-stripping reaction $Ca^{40}(d,p)Ca^{41}$. For this reason, considerable attention was paid in the analysis to questions such as the existence of ambiguities in the choice of optical-model potential, and to the possibility of finding a potential whose parameters show at most a slow variation over this energy range. At the same time, of course, an attempt to understand the observed scattering is of interest in itself.

Many deuteron-scattering experiments have been analyzed recently, and optical-model potentials have been found whose parameters show systematic trends through the periodic table.[1,2] Although data have been taken at a number of energies, there have been very few systematic measurements of the scattering as a function of energy.

II. EXPERIMENTAL METHOD AND RESULTS

Thin natural Ca targets (96.97% Ca^{40}) were bombarded with 7.0-, 8.0-, 9.0-, 10.0-, 11.0-, and 12.0-MeV deuterons from the Argonne tandem Van de Graaff. The targets were thin rolled foils of Ca metal about 1 mg/cm² thick, mounted in the center of a scattering chamber 18 in. in diameter, which was developed by Braid and Heinrich. Elastically scattered deuterons were detected in a commercial surface-barrier Si detector mounted on an arm whose angular position could be remotely controlled with a precision better than 0.2°. Measurements were made at 5° intervals over an angular range from 10 to 165°. The incident beam was defined by two circular apertures $\frac{1}{16}$ in. in diameter and fixed 11 in. apart, followed by a slightly larger antiscattering aperture. The collimating system was electrically insulated, and the beam was always focused so that less than 25% was intercepted by any of the slits.

To avoid possible inaccuracies due to microscopic nonuniformities in the targets, all angular distributions were measured relative to a monitor counter fixed at

† Work performed under the auspices of the U. S. Atomic Energy Commission.

[1] E. C. Halbert, Nucl. Phys. **50**, 353 (1964).
[2] C. Perey and F. Perey, Phys. Rev. **132**, 755 (1963).

90°. To obtain accurate absolute cross sections, the targets were bombarded by a 5-MeV alpha-particle beam from the tandem, with no other change in the experimental arrangement. The scattering of these alpha particles from Ca was assumed to be pure Rutherford scattering, so the absolute deuteron elastic-scattering cross sections could be determined relative to this known cross section. Defocused beams were used for all of these absolute measurements to insure uniform illumination of the target. It is believed that the measured absolute cross sections are accurate to $\pm 5\%$ or better.

At each angle, the spectrum of pulses from the counter was recorded in a 100-channel quadrant of a 400-channel pulse-height analyzer. A typical spectrum at 120° and $E_d = 9.0$ MeV is shown in Fig. 1. The reverse bias on the counter was kept low enough that the pulses from reaction protons were much smaller than those from scattered deuterons, and suitable absorbers intercepted the very small number of alpha particles from the target. The spectra were punched onto IBM cards and were reduced to center-of-mass cross sections and "ratios to Rutherford" by a suitable computer program.

Difficulty was encountered at angles $\leqslant 45°$ because of the inevitable oxygen contamination of the Ca targets. To determine the yield due to Ca alone, the yield from oxygen was subtracted by means of an iterative procedure which involved measurements with two targets with different relative amounts of oxygen contamination. An excitation curve at 120° was measured from 7.0 to 9.5 MeV to determine if the scattering cross section varies smoothly and slowly with energy. This result is shown in Fig. 2. It is evident that some fluctuations are observed, but they are small and become less prominent as the deuteron energy is increased.

The measured absolute differential cross sections for elastic deuteron scattering from Ca are listed in Table I. These values, which are believed accurate to $\pm 5\%$, form the basis of the analysis which follows.

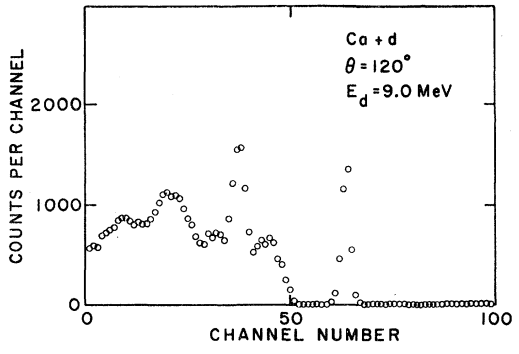

FIG. 1. Pulse-height spectrum of deuterons elastically scattered from the Ca target at 120° to the beam for a deuteron energy of 9.0 MeV. The zero of energy has been suppressed to facilitate the data collection.

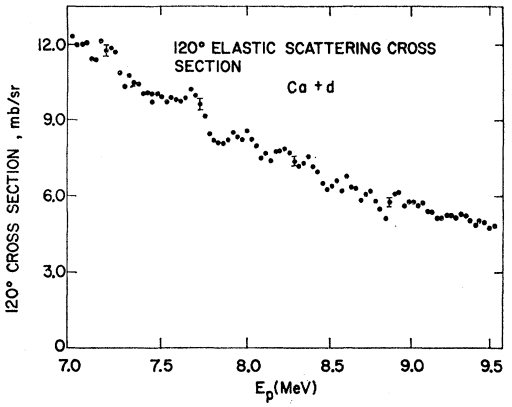

FIG. 2. 120° excitation function for elastic deuteron scattering from calcium. Statistical errors are shown by error bars on representative points.

III. OPTICAL-MODEL ANALYSIS

The complex optical-model potential used in the present analysis allowed the use of both volume and surface absorption, and was of the form

$$U(r) = -V(e^x+1)^{-1} - i(W-4W_D d/dx')(e^{x'}+1)^{-1} + U_c(r), \quad (1)$$

where

$$x = (r-r_0A^{1/3})/a,\ x' = (r-r_0'A^{1/3})/a',$$

and U_c is the Coulomb potential arising from a uniform charge of radius R_c, i.e.,

$$U_c(r) = \begin{cases} (Ze^2/2R_c^2)(3-r^2/R_c^2), & r<Rc \\ Ze^2/r, & r \geqslant R_c. \end{cases}$$

The value $R_c = 1.3A^{1/3}$ was used. The term in W in Eq. (1) represents volume absorption, while the term in W_D represents surface absorption. It is known from other work[1,2] that it is possible to produce the same scattering in this energy range with either volume or surface absorption. Hence the present analysis considered only one or the other, with most emphasis on the surface form.

The analysis was carried out by use of an automatic parameter-search program[3] coded for the IBM-7090 at Oak Ridge. This adjusts the parameters of the potential so as to minimize the deviation between experimental and theoretical cross sections. The measure of deviation used is

$$\chi^2 = \sum_{i=1}^{N} \left(\frac{\sigma_{\text{th}}(\theta_i) - \sigma_{\text{exp}}(\theta_i)}{\Delta\sigma_{\text{exp}}(\theta_i)} \right)^2, \quad (2)$$

where N is the number of experimental points, and the $\Delta\sigma$ are a set of weighting factors chosen to be approximately equal to the estimated experimental errors (10% for the smallest angle and 5% for all other angles). Any

[3] R. M. Drisko (unpublished notes). Some details of the procedure are given in Ref. 1.

TABLE I. Absolute differential cross sections in mb/sr for deuteron elastic scattering from calcium.[a]

c.m. angle	E_d (MeV) 7.0	8.0	9.0	10.0	11.0	12.0
10.5	147 620	118 850	88 860	64 310	51 240	41 570
15.7	29 170	23 620	16 130	12 640	9971	7640
21.0	8134	6489	4980	4198	3098	2431
26.2	3207	2536	2090	1433	984	779
32.4	1300	1182	800	533	358	216
36.6	734	507	345	221	140	98.8
41.8	402	268	198	149	110	87.8
47.0	243	182	155	131	103	82.5
52.2	178	141	123	107.3	83.6	62.2
57.3	142	113.9	104	82.8	62.3	42.9
62.5	98.9	75.6	66.4	48.2	45.4	25.1
67.6	71.6	46.2	39.4	28.0	20.2	15.6
72.7	46.8	27.0	22.5	16.4	12.6	9.88
77.8	28.6	16.2	12.9	9.87	8.13	5.91
82.8	19.9	12.1	9.99	7.74	5.93	4.03
87.9	15.4	10.9	9.22	6.91	5.45	3.84
92.9	15.4	11.4	9.40	6.68	5.30	4.66
97.9	16.0	12.3	9.04	6.38	5.84	5.39
102.8	16.8	13.1	8.60	6.26	5.96	5.65
107.8	16.1	13.1	8.38	6.16	5.55	5.07
112.7	16.3	11.7	7.42	5.48	4.84	4.00
117.6	14.8	10.5	6.93	4.58	3.75	2.89
122.5	12.5	9.2	5.64	3.63	2.74	1.96
127.3	10.7	8.02	4.74	2.72	1.86	1.40
132.2	8.70	6.92	3.59	1.95	1.16	1.24
137.0	7.36	6.23	2.93	1.38	0.867	1.15
141.8	5.27	5.80	2.90	1.88	1.17	1.64
151.4	4.66	6.64	3.83	2.62	1.90	2.00
156.2	4.67		5.03	4.14	2.66	2.32
161.0	4.62		6.76	5.72	3.62	2.60
165.7	4.81		8.11	6.94	4.25	2.69

[a] The standard deviations in the cross sections are believed to be $\pm 10\%$ for $\theta \leq 15°$ and $\pm 5\%$ elsewhere.

number of the parameters of potential (1) may be subjected to search in this way.

Preliminary studies made it clear that neither volume nor surface absorption could give good fits to experiment with a potential that had the same radius for real and imaginary parts. It is necessary to allow the absorptive potential to extend to considerably larger radii than the real potential. Further, the diffuseness parameters a and a' have to be made different to give good fits. Thus, if we restrict ourselves to pure surface absorption ($W=0$) or pure volume absorption ($W_D=0$), the potential (1) is specified by six adjustable parameters. In later sections we consider the effects of augmenting the potential (1) with a spin-orbit coupling and also a polarization potential.

IV. "BEST-FIT" POTENTIALS

In this section we consider fitting the data by allowing all six parameters to vary at each energy. It is already known[1,2] that there exist ambiguities in the

TABLE II. Parameters for potentials which give minimum χ^2 for 11-MeV data.

Potential	V (MeV)	r_0 (F)	a (F)	W (MeV)	W_D (MeV)	r_0' (F)	a' (F)	σ_R (mb)	$(\chi^2/N)^{1/2}$
X	32.5	0.943	0.905		5.6	1.703	0.691	1353	1.868
XP[a]	32.5	0.943	0.818		5.6	1.697	0.690	1358	1.852
Y	72.4	0.936	0.943		11.8	1.511	0.542	1163	2.007
YN[b]	73.3	0.936	0.896		11.0	1.516	0.554	1145	1.844
Z	120.7	0.966	0.846		16.4	1.479	0.492	1133	2.205
ZN[b]	124.5	0.951	0.819		15.1	1.479	0.506	1112	2.070
ZP[a]	120.8	0.964	0.840		16.5	1.476	1.489	1128	2.128
$Z3S$[c]	122.1	0.960	0.832		13.8	1.484	0.529	1152	2.000
G	176.9	1.002	0.769		21.0	1.466	0.453	1117	2.261
F	240.0	1.040	0.707		26.4	1.462	0.415	1104	2.281
J	303.6	1.091	0.651		34.5	1.468	0.368	1092	2.281
K	406.5	1.069	0.633		37.8	1.468	0.359	1095	2.292
L	459.6	1.154	0.573		51.5	1.489	0.304	1085	2.298
VY	68.0	0.991	0.870	5.19		0.970	0.267	1113	2.000
VZ	108.6	1.061	0.773	7.77		1.837	0.314	1091	2.196

[a] Polarization potential with $\alpha=0.52$ included. [b] Data multiplied by 1.1 before searching. [c] Includes vector spin-orbit coupling of 4.74 MeV.

potentials for deuterons; several discrete sets of parameters give very closely the same scattering. This point was studied in detail in the present analysis of the data at 11 MeV. With surface absorption only ($W=0$), the eight potentials X, Y, Z, G, F, J, K, and L, whose parameters are listed in Table II, were found to minimize χ^2. It seems probable that even deeper potentials may be found. The values of the root mean χ^2 given in column 10 of Table II indicate that all eight potentials fit the data equally well. This is confirmed by Fig. 3, where the ratios to Rutherford of the predicted cross sections for the first five are compared with experiment. The other three give very similar results. Only X gives significantly different predictions; the others are closely equivalent. We return to this point later. Although the X potential has a slightly smaller χ^2, a subjective visual judgment might favor the other group. Potentials closely corresponding to X, Y, and Z were found for the other energies; others were not looked for. Only at 12 MeV is there any significant difference between the quality of fits obtained, and at this energy the X-type potential is favored. The results for the Z-type potentials are compared with experiment in Fig. 4.

It has been found previously[1] that to each surface-absorption potential there is a corresponding volume-absorption potential with a closely similar real part. This is the case here also; parameters for two such potentials VY and VZ, which are the analogs of Y and Z, are included in Table II. The predicted cross sections are compared with experiment in Fig. 5. Table I shows

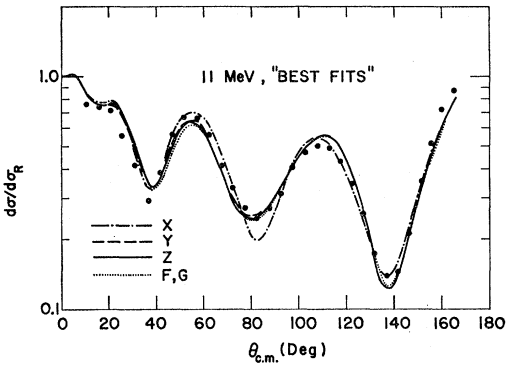

FIG. 3. Comparison of the 11-MeV data with 5 of the "best-fit" surface absorption potentials, illustrating the basic optical-potential ambiguity. The two volume absorption potentials V and VZ shown in Fig. 5 are essentially identical to these also.

that the values of χ^2 for VY and VZ are almost identical with those for Y and Z, and comparison of Figs. 3 and 5 shows the scattering to be almost identical also.

It is also worth noting from Table II that the predicted reaction (absorption) cross section σ_A are closely similar for the various potentials. Except for potential X, they are all included by 1124±39 mb, while X predicts a value some 20% larger.

It is clear from Figs. 3, 4, and 5 that the optical-model fits, though good, are by no means perfect; they deviate from experiment by 10 or even 20% at some angles. This may be due to unsuspected experimental

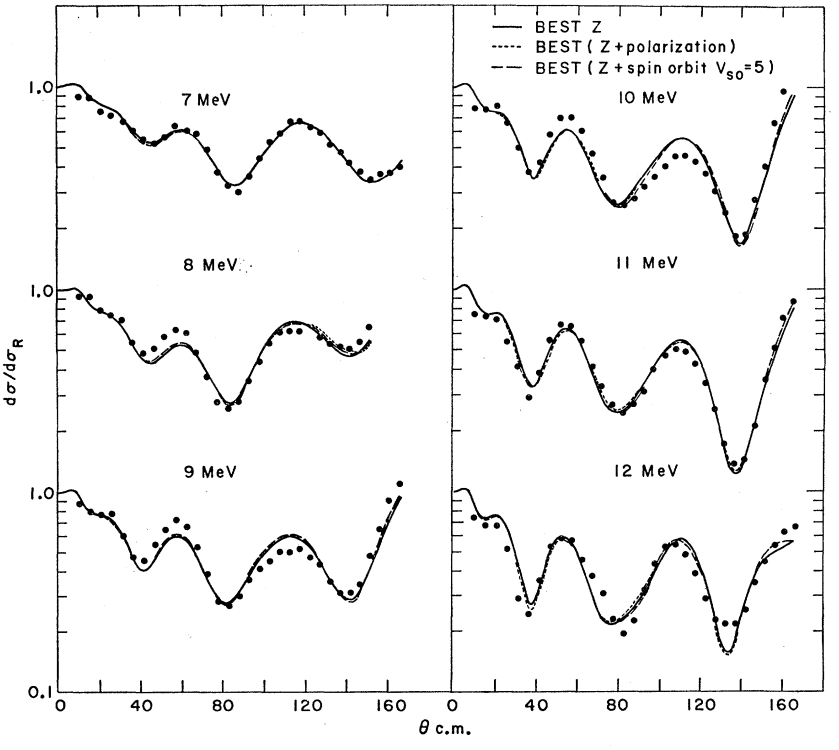

FIG. 4. Comparison of the measured σ/σ_R with predictions of best-fit potentials of the Z type for all energies measured. Parameters are as given in Table III. The dashed curves are the results when a polarization potential is included.

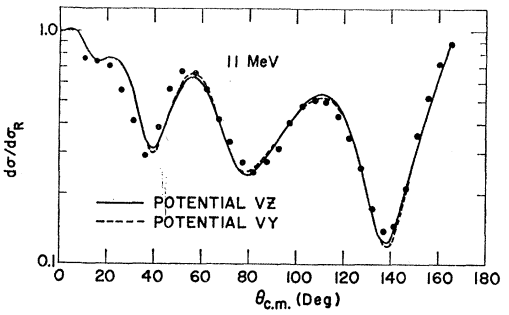

FIG. 5. Predictions of two volume absorption potentials (analogs of V and Z) compared to the 11-MeV data.

errors, to insufficient averaging over compound-nucleus fluctuations, or to inadequacies in the model itself. One example of the latter is that the particular functional form of Eq. (1) omits the possibility of the deuteron experiencing a polarization potential in the external Coulomb field.[4] This is discussed in Sec. VI.

In order to test the effects of a possible systematic error in the absolute cross sections, the data points taken at 11 MeV were increased by 10%, and optimum fits for potentials of type Y and Z were found again. These parameters (labeled YN and ZN) are also shown in Table II. Very little change has been produced; the 15% decrease in χ^2 is probably not significant.

In a recent analysis for medium and heavy nuclei,[2] C. and F. Perey recommended four sets of potential parameters which give a good account of the scattering of deuterons with energies of 10 to 22 MeV. These sets specify fixed radii and diffuseness parameters. They found that it was not possible to obtain good fits to the scattering from Ca at[5] 11.15 or[6] 12.1 MeV with these parameters, so it was of interest to apply them to the present data also. We found similar results; although definite minima in χ^2 are found when V and W_D are varied, the fit to the data is distinctly poor. The full curve in Fig. 6 is an example of this at 11 MeV. Their set-B parameters ($r_0=1.15$, $a=0.81$, $r_0'=1.34$, $a'=0.68$) were used, and a χ^2 minimum was found with $V=84.1$ MeV and $W_D=27.0$ MeV. The characteristic failure of the theoretical curve is the appearance of a double peak at about 60°, instead of the single peak observed experimentally. The curves predicted by the other sets of parameters are almost identical with that for set B. The previous analysis[1,2] of the 11.15- and 12.1-MeV data suggested that the main fault of the recommended parameters was in having too small a radius r_0' for the absorptive well. This is further evidenced by the values given in Table I. Indeed, examination of the "best-fit" parameters[1,2] obtained for the 11.8-MeV data[7] on heavier elements reveals a definite trend for r_0' to increase for lighter nuclei. This trend, which may be expressed roughly by

$$r_0'=a+(b/A^{1/3})$$

(where $a\approx 1$ F and $b\approx 2$ F), could be interpreted as an effect of the size of the deuteron. To demonstrate this further, after the optimum values of V and W_D were found with the shape parameters fixed at the values given by the Pereys, a further search was made in which V, W_D, and r_0' were allowed to vary. The optimum fit was obtained with little variation in V, but with a considerable increase in r_0' and a compensating decrease in W_D. (For set B, shown as the long-dashed curve in Fig. 6, the optimum values are $V=86.9$, $W_D=12.6$, and $r_0'=1.57$.) Although the over-all fit is considerably improved, the incipient double peak is still evident around 60°. Finally, allowing the imaginary diffuseness a' to vary eliminated the double peak. The optimum values obtained with set B as the starting point are then $V=92.7$ MeV, $W_D=20.3$ MeV, $r_0'=1.52$ F, and $a'=0.416$ F. The corresponding predicted cross section is shown as the short-dashed curve in Fig. 6. (These imaginary parameters differ slightly from those in Table II because the imaginary potential has to partially compensate for the constriants imposed on the real potential.) The same procedure applied to the other sets of parameters of Perey led to curves almost identical to those of Fig. 6; in each case the optimum fit is obtained with $r_0'\approx 1.5$ F and $a'\approx 0.4\pm 0.05$ F. Of course, when the shape (r_0 and a) of the real part of the potential is allowed to vary, the parameters converge to the values given in Table II (sets A and C to potential Y, sets B and D to potential Z).

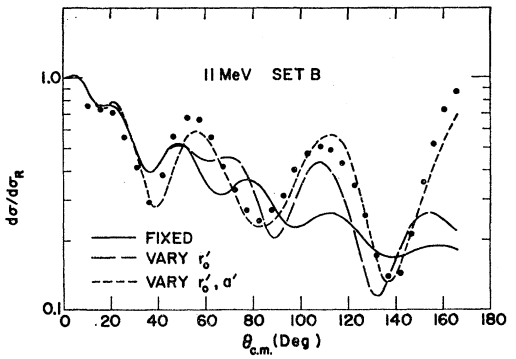

FIG. 6. Comparison of 11-MeV data with predictions of "set B" potential parameters suggested by Perey. For curve labeled "fixed," only V and W_D were varied to give "best fit"; next r_0' was varied also; and finally, both r_0' and a' were allowed to vary. Perey's sets A, C, and D parameters give very similar results.

The finding that the real radius parameter r_0 is smaller, and the real diffuseness a is larger, than is found for heavier nuclei[1,2] is also significant. The "best-fit" parameters for these nuclei also show a slight trend for r_0 to increase, and for a to decrease, with increase in A,

[4] C. F. Clement, Phys. Rev. **128**, 2728 (1962).
[5] M. Takeda, J. Phys. Soc. Japan **15**, 557 (1960).
[6] A. Strzalkowski, Phys. Letters **2**, 121 (1962).
[7] G. Igo, W. Lorenz, and U. Schmidt-Rohr, Phys. Rev. **124**, 832 (1961); T. Becker, U. Schmidt-Rohr, and E. Tielsch, Phys. Letters **5**, 331 (1963).

and this trend has been confirmed by an analysis of the scattering from lighter nuclei which is currently underway.

As mentioned above, optimum fits with potentials of types X, Y, and Z were also obtained for the data at the other energies. Parameters for the Z-type potentials are given in Table III, together with their rms values of χ^2. The fits obtained with the other potentials are as good as those with the Z type (shown in Fig. 4), and also those obtained at 11 MeV, and shown in Fig. 3. The parameters show a smooth variation for energies from 9 through 12 MeV, but some fluctuation is apparent at 7 and 8 MeV. It is believed that the *relative* errors between cross sections at different energies are less than 10%, so it seems more likely that the deviations at the lower energies are due to imperfect averaging over compound-nucleus states. However, it is worth noting that such errors in absolute cross sections could have an appreciable effect on the optimum optical-model parameters.

V. PHASE SHIFTS AND EQUIVALENT POTENTIALS

It is interesting to see what (complex) phase shifts, or scattering-matrix elements, are predicted by the optical model, and to what extent this analysis of the data provides a unique set of phase shifts. First, Fig. 7 shows the magnitude and phase of the scattering-matrix elements (reflection coefficients)

$$\eta_L = |\eta_L| \exp 2i\delta_L$$

for some of the "best-fit" potentials at 11 MeV given in Table II. Values for the other potentials are very similar to those shown for Y, Z, and F and exhibit systematic behavior; for example, the results for G fall between those for Z and F, those for VY are close to those for Y, etc. This similarity is in accord with the fact that they predict very similar angular distributions. On the other hand, the values of η_L for potential X deviate significantly from the rest, and, as Fig. 3 shows, so does its predicted angular distribution. Since there is little to choose between the quality of fits to the data with these two sets of values of η_L, Fig. 7 gives some measure of the uncertainty in the η_L obtained this way. It then becomes of interest to carry out a direct phase-shift analysis of the experimental data; this is being undertaken. The two sets of η_L have similar characteristics, particularly the odd-even structure for small values of L. Indeed, it is the lack of this structure for small L which prevents the potentials recommended by the Pereys from giving a dood fit to the data (see Fig. 6). Increasing the radius of the absorptive potential immediately introduces this structure. Very similar structure is observed at the other energies also, and the relation between the η_L for the X and other types of potential is preserved. The same ambiguity had been noted previously for Ca at 11.15 MeV.[1] Figure 8 shows the η_L at the various energies for the optimum type-Z potentials.

TABLE III. Parameters for potentials of Z type which give minimum χ^2 at each energy.

E	V (MeV)	r_0 (F)	a (F)	W_D (MeV)	r_0' (F)	a' (F)	σ_A (mb)	$(\chi^2/N)^{1/2}$
7	145.1	0.803	0.987	9.6	1.718	0.578	1165	0.894
7[a]	145.4	0.798	0.977	9.4	1.724	0.595	1175	0.890
7[b]	140.4	0.832	0.973	9.0	1.723	0.591	1161	0.854
8	109.4	1.011	0.977	24.4	1.658	0.343	1027	1.794
8[a]	124.2	0.908	1.007	21.8	1.654	0.371	1045	1.852
8[b]	118.9	0.949	0.993	20.6	1.657	0.372	1042	1.694
9	114.3	0.974	0.932	17.1	1.611	0.453	1143	2.342
9[a]	119.9	0.945	0.929	17.0	1.599	0.452	1127	2.434
9[b]	121.1	0.937	0.943	14.8	1.624	0.474	1160	2.342
10	124.8	0.924	0.920	15.4	1.559	0.498	1189	2.878
10[a]	123.6	0.932	0.905	16.1	1.545	0.483	1161	2.974
10[b]	134.0	0.876	0.927	13.3	1.562	0.520	1194	2.706
11	120.7	0.966	0.846	16.4	1.479	0.492	1133	2.205
11[a]	120.8	0.964	0.841	16.5	1.476	0.489	1128	2.128
11[b]	122.2	0.960	0.836	16.0	1.484	0.521	1147	1.968
12	112.8	1.021	0.846	19.8	1.471	0.444	1144	3.112
12[a]	111.6	1.029	0.840	20.8	1.466	0.429	1132	2.982
12[b]	110.4	1.036	0.840	17.1	1.485	0.462	1169	2.706

[a] Polarization potential with $\alpha = 0.52$ included.
[b] Vector spin-orbit coupling with $V_s = 5$ MeV, $W_s = 0$, included.

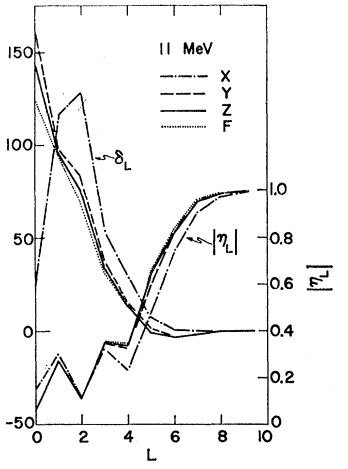

FIG. 7. Magnitude and phase of reflection coefficients η_L for "best-fit" potentials at 11 MeV, $\eta_L = |\eta_L| \exp 2i\delta_L$. The results for potential G fall between those for F and Z.

It is well known that some uncertainties in optical-model parameters arise because the effects of varying two or more parameters are often correlated. For example, small variations in V and r_0 may be made without substantially worsening a fit, provided Vr_0^n is kept constant. For 11-MeV deuterons on Ca, n is approximately 1.76 for potential X, and then decreases slowly as the potentials get deeper, from about 1.40 for potential Y to 1.26 for potential G, and so on. Two other cases of approximate relations between pairs of parameters were observed for the imaginary part of the Z potential at 11 MeV. Namely, for small variations, we have

$$\delta W_D/\delta r_0' \approx -63 \pm 7 \text{ MeV/F}$$

and

$$\delta W_D/\delta a' \approx -33 \pm 7 \text{ MeV/F}.$$

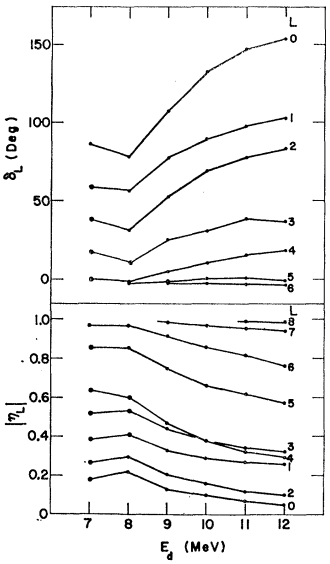

FIG. 8. Reflection coefficients (or scattering matrix elements) η_L obtained from the potentials of type Z when all the parameters are varied to obtain the best fit at each energy. The η_L obtained from potentials of type Y are closely similar. The phase δ_L is given by $\eta_L=|\eta_L|\exp(2i\delta_L)$.

Otherwise, the variations of the parameters are coupled 3 or more at a time. Presumably, analogous results may be obtained for the other potentials and at other energies.

In addition to these minor uncertainties, we have already noted that major ambiguities exist, as typified by the various sets of optimum parameters listed in Table I. Some of the corresponding potentials are plotted in Fig. 9. They share no obvious and simple property, except possibly that the various imaginary parts have roughly the same value at about 6.5 F. However, it has already been remarked[8] that one can understand the relationship between these various equivalent potentials in terms of the WKB approximation to the term which the nuclear interior contributes to the reflection coefficient η_L for small L.[9] This contribution is

$$\eta_L^{(\mathrm{in})}=\exp 2iS_L,$$

where

$$S_L=C_L+\int_{rL}^{\infty}K_L(r)dr$$

and

$$K_L^2(r)=(2M/\hbar^2)[E-U(r)-(\hbar^2/2Mr^2)L(L+1)].$$

Here C_L is a constant, while r_L is the classical turning point. Clearly, if $U(r)$ is changed so that S_L is increased by π, this contribution to η_L is unchanged. While this can be done exactly for one value of L, the η_L for neighboring values of L will be approximately unchanged also. It is found that the successive types of potential in Table II are related in exactly this way, each changing just enough for S_L to increase by π, for the lowest 5 or 6 values of L. The relation begins to break down for $L=5$, and reflection from the surface begins to dominate for larger L. The X potential is a partial exception to this rule; the differences between the phases S_L for X and Y differ from π by roughly 10% even for small L. This is enough to account for the differences between the cross sections they predict (Fig. 3). It is clear that physically X is related to the other potentials in this way; the deviations from π are due to X being fairly shallow, and to the consequent difficulty in satisfying the $\Delta S_L=\pi$ rule for all the low-L partial waves simultaneously. Indeed, for potential X, the $L=4$ wave does not penetrate and experience significant reflection from the interior. The same difficulties appear to preclude an even shallower potential that would fit the data; a broad minimum in χ^2 can be found for a potential with a depth of about 6 MeV, but it was not possible to find a good fit here. At the other extreme of very deep potentials, the limitation would appear to be the increasing difficulty in satifsying the $\Delta S_L=\pi$ rule for the nuclear-interior contribution to η_L, while at the same time not changing the reflection from the surface. It will be noted that the optimum χ^2

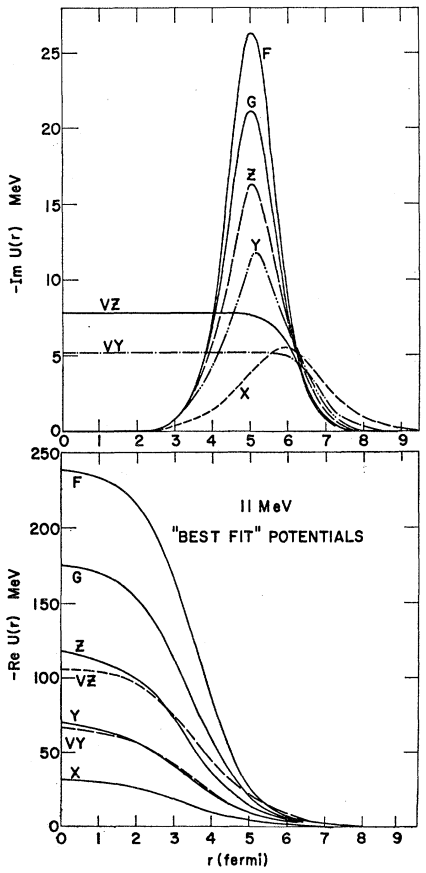

FIG. 9. The radial distribution of the real and imaginary parts of the potentials which best fit the 11-MeV data.

[8] R. M. Drisko, G. R. Satchler, and R. H. Bassel, Phys. Letters 5, 347 (1963).
[9] N. Austern, Ann. Phys. (N. Y.) 15, 299 (1961).

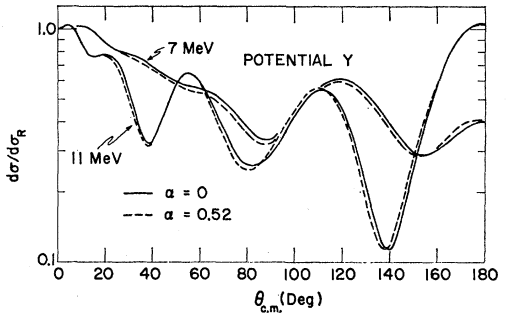

FIG. 10. Effect of addition of a deuteron polarization potential to the Y potential at 7 and 11 MeV. The solid curve shows the best-fit predictions without polarization. The dashed curve indicates the effect of addition of the polarization potential with no additional adjustment of parameters.

in Table II becomes progressively (but slowly) larger as the well depth increases.

The $\Delta S_L=\pi$ rule relating consecutive potentials corresponds to including just one extra half-wavelength in the interior for the low-L waves. This has been demonstrated previously[2] by explicitly calculating the various partial-wave radial functions for a series of equivalent potentials. In the total wave function, this shows up mainly as a movement of the focal peak towards the nuclear center as the well depth increases.[1,2] Of course, the wave functions *outside* the nucleus are closely similar, inasmuch as the potentials were chosen to reproduce the same asymptotic values, that is, the same scattering. These properties are clearly of importance when the waves are used in distorted-wave calculations of direct reactions.[9,10] Their consequences for the $Ca^{40}(d,p)$ reaction are considered in more detail in the following paper.

VI. POLARIZATION POTENTIAL

The deuteron will be stretched (polarized) by the Coulomb field of the nucleus, and thereby acquire a polarization potential. It has been suggested that under some circumstances this is the dominant mechanism responsible for deuteron scattering.[4] Since the polarizing allows the center of mass of the deuteron to approach the nucleus more closely than its center of charge, this potential is attractive. The main contribution is expected to be due to the dipole interaction, and has the form

$$U_{\rm pol}=-Z^2e^2\alpha/2r^4, \quad r>R_c, \tag{3}$$

where α is the deuteron polarizability. Estimates of α center around 0.5; the present calculations used $\alpha=0.52$, corresponding to $U_{\rm pol}=-150/r^4$ for Ca^{40}, where $U_{\rm pol}$ is in MeV and r is in F. Although such a potential is very weak, the cumulative effect of the long tail need not be negligible. In fact, however, Fig. 10 shows that the effect of simply adding this term to potential Y at deuteron energies of 7 and 11 MeV is quite small. When the optical-potential parameters are varied to regain the optimum fit to the experimental data in the presence of $U_{\rm pol}$, quite small changes are required, as indicated in Table III for $E_d=7-12$ MeV for the Z-type potentials, and in Table II for 11 MeV and both X and Z potentials. The corresponding cross sections for the Z type are shown as dotted curves in Fig. 4.

It should be noted, however, that the form of potential (3) and the value of α used are strictly valid only if the scattering is adiabatic with respect to the internal motion of the deuteron.[4] Further, it neglects the possibility of real breakup of the deuteron in the electric field, which would lead to an imaginary component of $U_{\rm pol}$.

VII. SPIN-ORBIT COUPLING

Another possible deficiency in potential (1) comes from omitting any spin-orbit coupling. There are several possible forms of spin-orbit coupling for spin-1 particles,[11] but here we consider only the effects of the well-known vector type. The term

$$U_{\rm so}=(\hbar/m_\pi c)^2(V_s+iW_s)\,(1/r)\,(d/dr)\,(e^x+1)^{-1}\mathbf{L}\cdot\mathbf{s}$$

was added to potential (1). The radius and diffuseness were taken to be the same as for the real potential. Figure 11 shows the results of including such a term with the Z-type potential for a deuteron energy of 11 MeV. The potential labeled $Z2S$ was obtained by allowing V, W_D, and V_s to adjust for an optimum fit, but fixing $r_0=1.0$ F, $a=0.87$ F, $r_0'=1.5$ F, and $a'=0.5$ F. W_s was put to zero. The search converged to the value $V=113.7$ MeV, $W_D=15.9$ MeV, and $V_s=4.74$ MeV, which are to be compared with the values $V=113.2$ MeV and $W_D=16.8$ MeV when $V_s=0$. When all the parameters were varied (keeping $V_s=4.74$), the optimum fit yielded the values labeled $Z3S$ in Table I. The gain in χ^2 is quite small. The vector polarizations

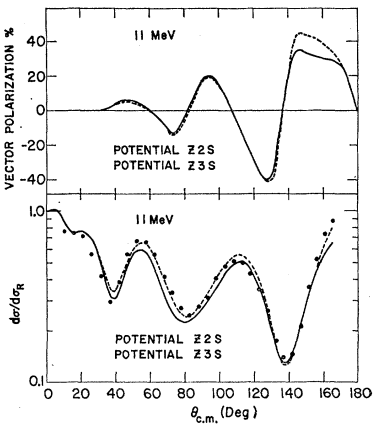

FIG. 11. Effect of vector spin-orbit coupling at 11 MeV. The lower curve shows fits to differential cross section for potentials $Z2S$, $Z3S$, while the upper curve shows predictions of these potentials for the vector polarization produced.

[10] G. R. Satchler, in *Proceedings of the Conference on Direct Interactions and Nuclear Mechanisms, Padua, Italy, September 1962* (Gordon and Breach Science Publishers, New York, 1963), p. 80; Proceedings of Symposium on Nuclear Spectroscopy with Direct Reactions, Chicago, 1964, ANL Report 6878 (unpublished).

[11] G. R. Satchler, Nucl. Phys. **21**, 116 (1960).

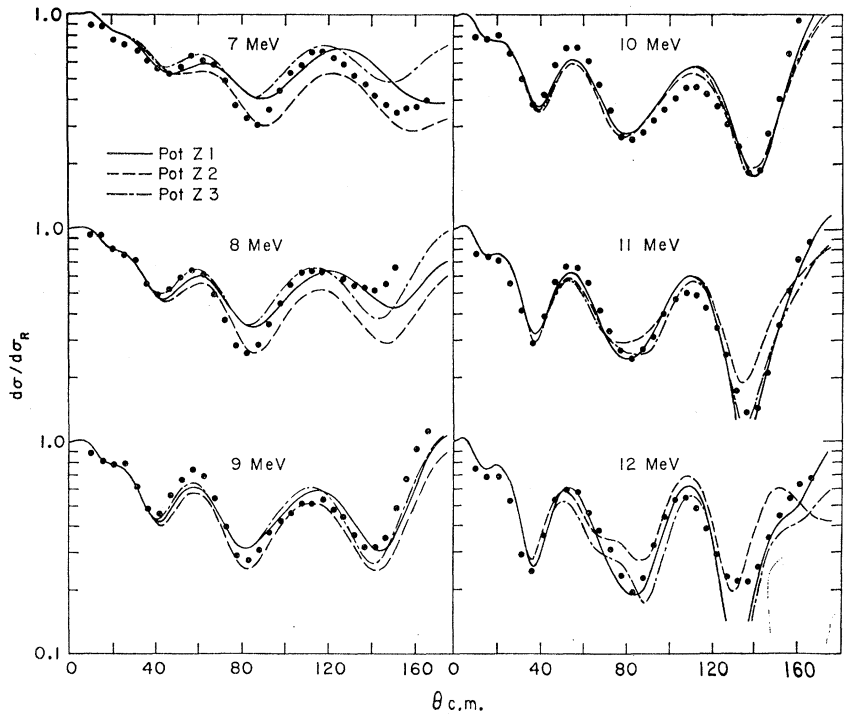

FIG. 12. Comparison of present data with predictions of the "averaged" optical potentials $Z1$, $Z2$, and $Z3$.

produced by these two potentials are also shown in Fig. 11.

Inclusion of an imaginary part $W_s \neq 0$, and allowing the radius and diffuseness to differ from those of the real central potential, led to no improvement. Similar conclusions were reached with spin-orbit coupling added to the X and Y potentials. We conclude, then, that the data at these energies gives no compelling reason to include spin-orbit coupling. Direct evidence for its existence must await polarization measurements such as those carried out at 22 MeV. The latter are consistent with a real spin-orbit coupling of strength about 6 MeV.[12] In view of this, and because of the interest in using the potentials in analyses of polarization measurements on deuteron stripping reactions, searches were made for optimum fits to the present data using potentials of type Z with a real spin-orbit coupling of strength $V_s = 5$ MeV, and radius and diffuseness equal to those of the real central potential. The results of this analysis are included in Table III. The predicted cross sections are shown as dashed curves in Fig. 4. While these are almost indistinguishable from the curves obtained without spin-orbit coupling, the values of χ^2 are consistently lower at each energy.

VIII. "AVERAGE" POTENTIALS

Some of the energy dependence of the values of the optimum parameters, as given in Table III for example, are due to the existence of approximate invariants, such as the Vr_0^n already mentioned. Others may be due to idiosyncracies in the data, both real and instrumental. Hence, it is of interest to attempt to find sets of averaged parameters, with at most a slow energy variation, that give the best over-all fit to the data. This is not easy to do in the absence of an automatic search routine that will optimize the fits to the data at all energies simultaneously. However, the following procedures were adopted for use with the Z-type potential. First, the real radius was fixed at $r_0 = 1.0$, and the diffuseness at $a = 0.9$, and several pairs of values for r_0' and a' were adopted. For each pair, the optimum values of V and W_D at each energy were determined. On the basis of this limited study, the values $r_0' = 1.55$ and $a' = 0.47$ were chosen. The optimum values of V were then close to 112 MeV at each energy, while the optimum values of W_D were about 17 MeV for energies of 10 to 12 MeV but tended to increase for the lower energies. Hence the values $V = 112$ MeV and $W_D = 18$ MeV were chosen. The corresponding cross sections are shown as potential $Z2$ in Fig. 12. The fits for the lower energies are not appreciably worse than those obtained with the optimum W_D. A similar study was made when a vector spin-orbit coupling with a fixed strength of 5 MeV was added to the Z-type potential. This resulted in an increase in the optimum value of V at each energy of approximately $\frac{1}{2}$ MeV, while the optimum W_D was decreased by roughly 1 MeV at the higher energy and remained unchanged at the lower energy.

Next the geometrical parameters r_0, a, r_0', and a' were taken one at a time and varied together with V

[12] J. Raynal, Phys. Letters 7, 281 (1963).

and W_D to find optimum fits. In most cases a reduction in χ^2 resulted, although there was no marked preference for varying any one of the parameters. However, the smoothest energy dependence, which resulted from varying r_0' while holding $r_0=1.0$, $a=0.9$, and $a'=0.5$, could be summarized by $r_0'=1.98-0.04\ E$. The optimum well depths (Fig. 13) were then closely given by $V=111$ and $W_D=9+0.65\ E$. The curves for this potential are shown as Pot $Z3$, Fig. 12, and the parameter values indicated by dashed lines in Fig. 13.

Finally, an attempt was made to summarize the best-fit parameters of Table II with at most a linear energy dependence. In Fig. 13 these parameters are plotted against the incident energy. In view of the approximate correlations (Sec. V) between variations in different parameters, the linear relations shown as full lines in Fig. 13 were chosen as reproducing the over-all energy dependence. In choosing these, somewhat greater weight was given to the higher energy fits. They correspond to

$$V=183-5.8E,\quad r_0=0.44+0.048E,\quad a=1.29-0.038E,$$
$$W_D=15,\quad r_0'=2.01-0.045E,\quad a'=0.5.$$

The predicted cross sections are shown as the full curves labeled Pot$Z1$ in Fig. 12. Only at 7 MeV is the fit to experiment appreciably worse than that with the parameters of Table III.

The energy variation of r_0' is close to that observed when the other geometrical parameters were kept fixed. It is tempting to suggest that this variation arises because a large part of the deuteron absorption is due to direct reactions. These occur mainly in the surface region; as the energy is reduced close to the Coulomb barrier, this region will move out to larger radii. However, it should be emphasized that the results reported in this section may be without *physical* significance.

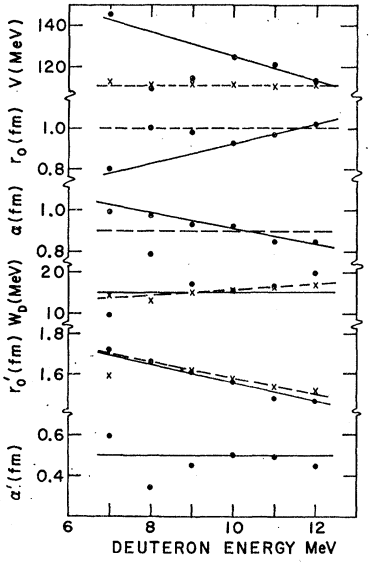

FIG. 13. Potential parameters plotted against energy. The dots correspond to the best-fit values of Table III when all parameters are varied. Crosses represent values obtained when only V, W_D, and r_0' are varied. The lines indicate average values chosen as described in the text.

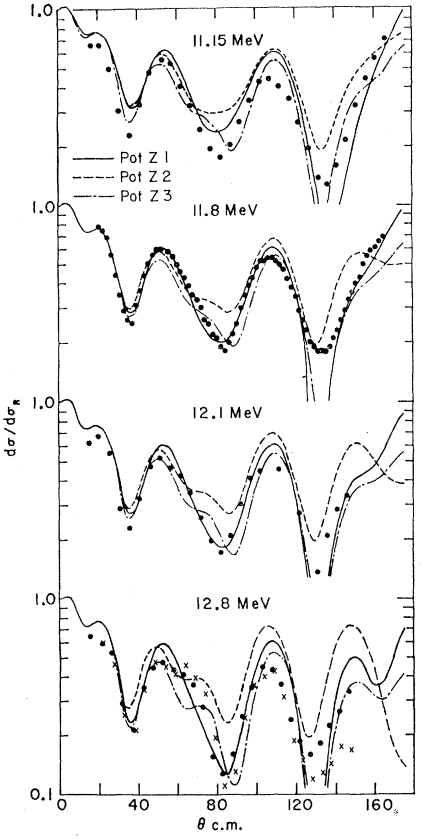

FIG. 14. Comparison of data obtained elsewhere in this energy region with predictions of the averaged optical potentials described in the text. The dots and crosses at 12.8 MeV (Ref. 6) represent data taken with two different targets. The theoretical curves shown with the 12.1- (Ref. 6) and 11.8-MeV (Ref. 7) data are those computed for 12 MeV.

Almost as good fits are obtained (by subjective judgment) when all the parameters are kept fixed; perhaps the results of this section serve rather to illustrate the danger of a blind application of the χ^2 criterion. The above three potentials serve as a useful summary of the fits found, although it would be unwise to extrapolate them much beyond the present energy range. They give a reasonable account of the other data available for this reaction, as shown in Fig. 14. It is interesting to note that the experimental curve at 12.8 MeV shows some evidence for the incipient double peak around 60° that occurs also in some of the theoretical curves.

IX. DISCUSSION

The elastic scattering of deuterons by Ca^{40} has been seen to vary rather smoothly with energy, although some structure is evident. It has also been shown that a good account of the data can be given by one or more optical potentials. It remains to comment upon the expected validlty of the optical-model description. The conditions of good averaging over "compound-nucleus" states and the absence of fluctuations with energy

appear to be reasonably well satisfied by the present experiment. Also, Ca^{40} being a closed-shell nucleus, it seems unlikely that inelastic scattering to any one state is strong enough to introduce explicit coupling effects which cannot be reproduced by the absorptive potential.[13] Whether the same is true for the deuteron-stripping channels is not clear. However, at 12 MeV the cross sections for the ground-state and first-excited-state (d,p) groups are still only a half or a third of the elastic cross section, even at backward angles, and become smaller at the lower energies. It does not seem likely that these channels could seriously affect the elastic scattering other than through simple absorption.

A more fundamental question is the applicability of the optical-model concept. The existence of an "optical model," in the formal sense, is guaranteed; but what one does not know *a priori* is the *physical* content of this statement. In particular, it is not guaranteed that the formal optical model can be represented by a simple central potential, let alone one having the particular functional form chosen here. At the very least, one would expect the potential to be nonlocal and probably L-dependent—that is, to be different for different partial waves. From this point of view, the success of simple optical-model potentials in fitting experimental data is quite remarkable. For nucleons, this perhaps implies that the simple potential concept is physically meaningful; the chief deficiency would then be the neglect of nonlocality, but it is known that this is taken into account effectively by allowing the potential parameters to vary with energy. It is clearly inadequate to describe the motion of a complex projectile inside the nucleus simply in terms of the motion of its center of mass, without explicit reference to its polarization and breakup (except insofar as this leads to absorption). Nonetheless, strongly absorbed particles with wavelength short compared with the nuclear size (typically 40-MeV alphas) are sufficiently semiclassical in behavior that an optical model has to do little apart from providing sufficient absorption and reproducing some nuclear "radius" and "surface diffuseness." Such scattering is dominated by reflection from the nuclear surface; conditions in the interior have little effect. The situation is quite different, however, for complex particles of longer wavelength, such as the deuterons whose scattering is discussed here. Reflection of low-L partial waves from the centrifugal barrier in the nuclear interior becomes important in addition to surface reflection, and leads to ambiguities in the potential, as noted here and elsewhere.[8] In other words, in these cases the question of the physical significance of the optical potential (and its associated wave functions) inside the nucleus becomes very relevant. Observation of the elastic scattering at most determines the asymptotic form of the scattered waves, but knowledge of the wave function close to, and inside, the target nucleus is required in direct-reaction calculations. This point will be considered further in the following paper.[1]

In the absence of other information of this type, choice between the various equivalent potentials must be made largely on the basis of prejudice. For example, if the potential inside the nucleus has any physical significance, it would be difficult to understand how its depth V could be much more than 100 MeV, or roughly the sum of the optical potentials for a free neutron and proton. Indeed, this point of view would single out the Z-type potential as the meaningful one.

ACKNOWLEDGMENTS

We are indebted to Dr. Edith Halbert for assistance with the preliminary analysis of the data, and to her and Dr. Perey for helpful discussions. We would also like to thank Frank Karasek for the preparation of the Ca targets, J. G. McShane and E. A. Kowalski for help in taking the data, and the Argonne tandem operating group.

[13] F. Perey and G. R. Satchler, Phys. Letters 5, 212 (1963).